Thermal Performance Analysis of a Downhole Coaxial Heat Exchanger for an Enhanced Geothermal System

T.V. Pham[1], Tsung-Sheng Sheu[2], Herchang Ay[1*], Hsiao-Kang Ma[3]

[1]Department of Mod and Die Engineering, National Kaohsiung University of Applied Sciences, Kaohsiung City, Taiwan
[2] Department of Mechanical Engineering, R. O. C. Military Academy, Kaohsiung City, Taiwan
[3] National Taiwan University, Taipei City, Taiwan

*corresponding author: herchang@gm.kuas.edu.tw

Abstract Based on available surveys, it has been shown that Taiwan has substantial geothermal potential. In order to exploit these renewable resources, it is necessary to study the performance of a Borehole Heat Exchanger (BHE) which plays a significant role in a geothermal power plant. Thus, the aim of this paper is to design, analyze performance and optimize the main parameters of a downhole coaxial heat exchanger for a water-dominated enhanced geothermal system (EGS). The paper consists of an analytical optimization and case studies of geothermal power plants in Nigorikawa (Japan) and Chingshui (Taiwan). A numerical optimization method is developed to extract maximum heat energy from the Earth about 2 km of depth which has medium-temperature geothermal fields. The entropy generation minimization analysis is performed in order to minimize the exergy destruction which is caused by the heat transfer irreversibility and the fluid friction irreversibility. Both the laminar and turbulent fully-developed flow regimes were investigated in optimization procedure. The optimal mass flow rate was established to minimize pumping power and maximize heat energy extraction. In addition, the coaxial pipe diameters of the downhole heat exchanger were determined to maximize the net power output. The geothermal temperature gradient and the geothermal outlet temperature were taken into account to observe the influence on the first and second-law efficiencies. The numerical results show that the geothermal flow regime, the mass flow rate, the geothermal injection and outlet temperature the most influencing factors to the coaxial geothermal heat exchangers (GHE) in thermal aspects. The assessment from the case studies show that the working fluid is significantly influent to the performance of geothermal power systems respect to first- and second-law efficiencies.
Keywords: binary geothermal power plant, coaxial heat exchanger, entropy generation minimization

1. INTRODUCTION

Geothermal energy is the energy contained as heat in the Earth’s interior. Below Earth's crust, there is a layer of hot and molten rock, called magma. Heat is continually produced in this layer, mostly from the decay of naturally radioactive materials such as uranium and potassium. The origin of this heat is linked with the internal structure of our planet and the physical processes occurring there. The amount of heat within 10,000 meters (about 33,000 feet) of Earth's surface contains 50,000 times more energy than all the oil and natural gas resources in the world. Despite the fact that this heat is present in huge, practically inexhaustible quantities in the Earth’s crust, not to mention the deeper parts of our planet, it is unevenly distributed, seldom concentrated, and often at depths too great to be exploited industrially [1]. Traditionally, the construction of geothermal power plants was restricted to areas near the edges of tectonic plates, volcanic sites, sedimentary hot sources as well as hot wet fractured granite. These regions contain subterranean hot water or steam reservoirs which facilitated hydrothermal energy flows either vertically by convection or horizontally through convection, advection and diffusion due to the difference in pressure of the extracted and rejected geothermal fluid [2]. The areas which have huge potential is the region around the Pacific Rim of Fire (consist of Central America, Japan, Indonesia, New Zealand, Philippines and the west of the United States), and the Great Rift Valley zones Iceland, East of Africa and Eastern Mediteranean.

Based on recent surveys, it is found that Taiwan also has large potential to exploit geothermal energy. A comprehensive exploration estimates that Taiwan has total shallow geothermal potential of up to 1000MW [3]. Therefore, exploiting geothermal energy has been listed as one of the major tasks of National Energy Program in Taiwan. A pilot 3 MW power plant was first operated in 1981 at Chingshui geothermal fields, located in Yi-Lan County, northeastern of Taiwan. The Chingshui, has potential of 61 MWe of geothermal electricity production, is one of the most promising geothermal resource in this country. However, this plant was terminated then in 1993 due to rapidly decrease of power generation from 1.2 MW to 0.2 MW. The reason for decline of power production was scaling based on the findings of carbonate and silica deposits inside well pipes [4]. The developing of new technology in recent years makes the scaling problems be overcome. In 2011, the National Science Council of Taiwan continuously operated new pilot binary power plant in Chingshui as a part of tasks in National Energy Program Phase II. These promotes for this study to design and analyze the performance of geothermal system in thermal aspect.

Among geothermal energy resources, the low- and medium-temperature are the most abundant. The binary power plants are the best energy conversion systems to exploit them, both from technical and environmental aspect.

In a binary cycle power plant, the heat energy from geothermal fluid (or brine) is transferred to the secondary working fluid which has low boiling point and high vapor pressure when compared to water at a given temperature (see Fig. 1). The secondary working fluid (now in the superheated phase) go into the turbine to generate electricity, then be cooled in the condenser before go to the pump and heat exchanger again. In part of geothermal fluid, the brine, after transferred heat energy to the working fluid, is then returned to the ground to recharge the reservoir [5].

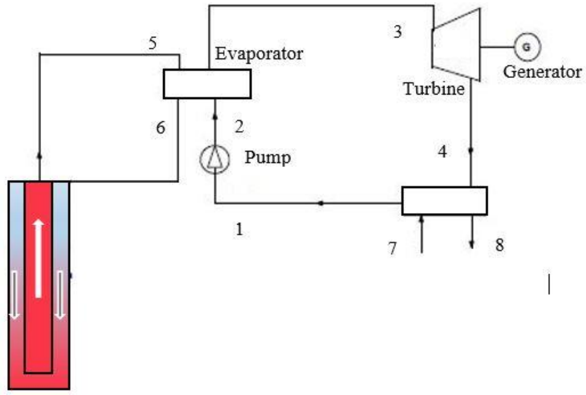

Fig. 1: A schematic of simple geothermal power plant

The downhole coaxial heat exchanger for an enhanced geothermal system is a closed-loop system which consists of two coaxial pipes. The geothermal fluid is continuously circulated through the Earth in a closed pipe system without directly contacting with the soil or hot rock. The cold water is pumped down through the annular space where this fluid stream is heated by the heat flux from the geothermal heat source through the outer pipe wall. The heated stream eventually returns in the inner pipe upward to the surface. The wall between upward stream and downward stream is insulated to minimize any potential loss of heat as the fluid returns to the surface.

There are a great number of studies have been conducted regarding to geothermal power plant fields and could be used in their exploitation for electricity production. Some studies focus on resource exploration and drilling techniques, while some others focus on energy conversion systems. Among these studies, Barbier (2002), Bertani (2005) and DiPippo (2008) provide analyses and an overview of the various technological solutions related to many aspects of geothermal energy. The energy and exergy efficiencies were used by Yari [6] to access various geothermal power plants. A study conducted by J.S. Lim et al. [7] proposed a model to investigate the energy extraction from fractured hot dry rock using first and second law analysis. Their study observed the process water be circulated through the narrow fractures created in the subterranean hot dry rock under the effect of transient conduction. Many of working fluids suitable for binary geothermal power plants were considered by Franco and partners [8]. It has illustrated that for given operating conditions, the power cycle is strongly affected by the geothermal fluid temperature at the inlet and outlet of the resource wells. A study by Yekoladio et al. [9] designs and optimizes the downhole coaxial heat exchanger to minimize the pumping power requirement for circulating the geofluid in the wells. The aim of these studies is reducing the cost of geothermal electricity production by optimizing the power cycle.

2. ANALYSIS

2.1 Assumptions

The following assumptions are considered in this study [6], [9]:

a) The geothermal power plants is operated under steady-state condition;

b) The underground gradient temperature increase linearly with the depth of the well. Therefore, a constant wall heat flux is assumed on the outer diameter of the coaxial heat exchanger;
c) The outer pipe of the downhole coaxial heat exchanger is highly conductive and the wall between upflowing hot stream and the downflowing cold stream is perfectly insulated. Hence, the heat transfer between the hot stream and cold stream is neglected;
d) The geofluid circulated in the downhole coaxial heat exchanger is in saturated liquid state.
e) The kinetic and potential energy changes are negligible;

2.2 Pressure loss in the downhole coaxial heat exchanger

The pressure drop per unit length of the pipe is given by Bejan [10] by:

$$\left(\frac{\Delta P}{L}\right) = f\,\frac{2\rho V^2}{D_h} \tag{1}$$

where $f = \left(\mathrm{Re}, \frac{k_s}{D_h}\right)$ is the friction factor.

The hydraulic parameter D_h is defined by

$$D_h = 4\frac{\text{cross-sectional area}}{\text{wetted perimeter}} \tag{2}$$

For the inner pipe flow, the D_h=D_i, the pressure drop per unit length of the pipe is expressed then by:

$$\left(\frac{\Delta P}{L}\right)_i = f_i\,\frac{2\rho V_i^2}{D_i} = f_i\,\frac{2\rho V_i^2}{D_o r} \tag{3}$$

Where the diameter ratio r is defined as:

$$r = \frac{D_i}{D_o} \tag{4}$$

Similarly, the pressure drop per unit length in the annular space of the downhole coaxial heat exchanger can be determined by

$$\left(\frac{\Delta P}{L}\right)_a = f_a\,\frac{2\rho V_a{}^2}{D_o(1-r)} \tag{5}$$

It should be mentioned that the hydraulic parameter D_h in the annular space is expressed by

$$D_h = D_o - D_i = D_o(1-\mathrm{r}) \tag{6}$$

Thus, the total pressure drop per unit length for the total two section of the coaxial pipe is

$$\left(\frac{\Delta P}{L}\right)_{total} = \left(\frac{\Delta P}{L}\right)_i + \left(\frac{\Delta P}{L}\right)_a = f_i\,\frac{2\rho V_i^2}{D_o r} + f_a\,\frac{2\rho V_a{}^2}{D_o\left(1-r\right)} \tag{7}$$

The conversation of mass (or continuity equation) can be written as

$$\sum_i(\dot{m}_i)_{out} = \sum_i(\dot{m}_i)_{in} = \dot{m} \tag{8}$$

Applying to the inner pipe

$$\dot{m}_{in} = \rho\frac{\pi D_i^2}{4}\cdot V_i = \rho\frac{\pi D_o^2 r^2}{4}\cdot V_i \tag{9}$$

Similarly, applying for the annular space

$$\dot{m}_{out} = \rho\frac{\pi D_o^2\left(1-r^2\right)}{4}\cdot V_a \tag{10}$$

Substitute (9-10) to (8)

$$V_i = V_a\cdot\frac{1-r^2}{r^2} \tag{11}$$

In the laminar fully-developed flow, the friction factors decreases inversely with the Reynolds number and be given by White [11]

$$f = \frac{16}{\mathrm{Re}} \tag{12}$$

$$\mathrm{Re}_a = \frac{\rho V_a D_o (1-r)}{\mu} \tag{13}$$

$$\mathrm{Re}_i = \frac{\rho V_i D_i}{\mu} = \frac{\rho V_a D_o}{\mu}\left[\frac{(1-r^2)}{r}\right] = \mathrm{Re}_a \frac{1+r}{r} \tag{14}$$

Substitute (11-14) to the equation (7)

$$\left(\frac{\Delta P}{L}\right)_{total} = \frac{32\mu V_a}{D_o^2}\left(\frac{1-r^2}{r^4} + \frac{1}{(1-r)^2}\right) \tag{15}$$

Equation (15) can be expressed by

$$\left(\frac{\Delta P}{L}\right)_{total} = 32\frac{\mu V_a}{D_o^2}\cdot \zeta_{lam} \tag{16}$$

where:

$$\zeta_{lam} = \left(\frac{1-r^2}{r^4} + \frac{1}{(1-r)^2}\right) \tag{17}$$

Equation (17) can be numerically minimized with respect to the diameter ratio r, to obtain the minimum total pressure drop and pumping power requirement.

$$r_{opt,lam} = 0.62 \tag{18}$$

In the large Reynolds number limit of fully turbulent, the friction factors of both the inner pipe and annular space are defined by Bejan [10]

$$f = 0.046\,\mathrm{Re}^{-1/5} \quad 10^4 < \mathrm{Re} < 10^6 \tag{19}$$

Substitute (4), (13), (14), (18) to the equation (7)

$$\left(\frac{\Delta P}{L}\right)_{total} = \frac{0.092\rho V_a^2\,\mathrm{Re}_a^{-0.2}}{D_o}\left[\frac{(1+r)^{-0.2}(1-r^2)^2}{r^{4.8}} + \frac{1}{1-r}\right] \tag{20}$$

Equation (20) can be expressed as

$$\left(\frac{\Delta P}{L}\right)_{total} = \frac{0.092\rho V_a^2\,\mathrm{Re}_a^{-0.2}}{D_o}\zeta_{turb} \tag{21}$$

where

$$\zeta_{turb} = \frac{(1+r)^{-0.2}(1-r^2)^2}{r^{4.8}} + \frac{1}{1-r} \tag{22}$$

Equation (22) can be numerically minimized respect to the diameter ratio to obtain minimum pressure drop

$$r_{opt,turb} = 0.72 \tag{23}$$

2.2 Entropy generation minimization analysis for the coaxial heat exchanger

The exergy balance for closed systems:

$$\frac{dE}{dt} = \sum_j \left(1 - \frac{T_o}{T_j}\right)\dot{Q}_j - \left(\dot{W} - \frac{dV}{dt}\right) - \dot{E}_D \tag{24}$$

Steady-state form:

$$\sum_j \dot{E}_{q,j} - \dot{W} + \sum_i \dot{E}_i - \sum_i \dot{E}_o - \dot{E}_D \tag{25}$$

The term $\dot{E}_D$ accounts for the destruction rate of exergy due to irreversibilities with in the system. The exergy destruction rate $\dot{E}_D$ is related to the entropy generation rate by:

$$\dot{E}_D = T_o \dot{S}_{gen} \tag{26}$$

The entropy generation rate per unit length is given by [9]

$$\dot{S}'_{gen} = \frac{\dot{m}C_p\Delta T}{T_m^2}\left(\frac{dT}{dx}\right) + \frac{\dot{m}}{\rho T_m}\left(-\frac{dP}{dx}\right) \tag{27}$$

Equation (27) can be written as [10]

$$\dot{S}'_{gen} = \dot{S}'_{gen,\Delta T} + \dot{S}'_{gen,\Delta p} \tag{28}$$

The first term in equation (28) accounts for the heat transfer irreversibility. The second term represents the fluid flow irreversibility as a result of fluid friction when the geothermal fluid is circulated in the pipes.

Since the heat transfer happens only near the outer wall of the annular space, the following equations is obtained from heat transfer principles [10, 12]

$$\Delta T = \frac{\dot{m}C_p}{h\pi D_o}\left(\frac{dT}{dx}\right) \tag{29}$$

$$Nu_a = \frac{hD_h}{k} = St \cdot \rho \cdot C_p \cdot V_a \tag{30}$$

$$h_a = St \cdot \rho \cdot C_p \cdot V_a \tag{31}$$

$$V_a = \frac{4\dot{m}}{\rho\pi D_o^2 (1-r^2)} \tag{32}$$

Substitute (29)-(32) into (27) and integrate along the length of the heat exchanger for a constant increment of the underground temperature with depth, the entropy generation rate per unit length can be written by

$$\dot{S}'_{gen} = \frac{\dot{m}C_p \operatorname{Re}_a \operatorname{Pr} D_o \left(1-r^2\right)}{4Nu_a T_m^2}\left(\frac{dT}{dx}\right)^2 + \frac{\dot{m}}{\rho T_m}\left(-\frac{dP}{L}\right)_{total} \tag{33}$$

Under the assumptions of uniform wall heat flux and in the fully developed laminar conditions, the Nusselt number is constant, independent of Reynolds number and Prandl number, axial location and be theoretically determined by Incropera et al. [12] as

$$Nu = \frac{hD_h}{k} = \frac{48}{11} \cong 4.36 \tag{34}$$

Substituting equation (16), (32) into the equation (33), the following equation was obtained

$$\dot{S}'_{gen} = \frac{\dot{m}C_p \operatorname{Re}_a \operatorname{Pr} D_o \left(1-r^2\right)}{17.44 T_m^2}\left(\frac{dT}{dx}\right)^2 + \frac{128\mu\dot{m}^2}{\pi\rho^2 T_m D_o^4 \left(1-r^2\right)}\zeta_{lam} \tag{35}$$

The dimensionless Reynolds number for the flow through straight annular space related with the mass flow rate can be determined by

$$\operatorname{Re}_a = \frac{4\dot{m}}{\pi\mu D_o (1+\mathrm{r})} \tag{36}$$

Eliminating D_o and substituting equation (36) to the equation (35), the following equation was obtained

$$\dot{S}'_{gen} = \frac{0.073\dot{m}^2 C_p \operatorname{Pr}}{\mu T_m^2}\left(1-r\right)\left(\frac{dT}{dx}\right)^2 + \frac{15.5\mu^5 \operatorname{Re}_a^4 \zeta_{lam}}{\rho^2 T_m \dot{m}^2} \cdot \frac{(1+r)^4}{(1-\mathrm{r}^2)} \tag{37}$$

Equation (37) was differentiated with respect to the mass flow rate of geothermal fluid and be minimized. The optimal mass flow rate of the geothermal fluid under laminar flow condition was determined for minimum entropy generation, thus maximum extracted heat energy for a given underground temperature gradient. The following equation were obtained

$$m_{opt,\mathrm{lam}} = 3.817 \operatorname{Re}_a \chi_{lam}^{0.25} \tag{38}$$

where,

$$\chi_{lam} = \frac{\mu^6 T_m}{\rho^2 C_p \operatorname{Pr}\left(\frac{dT}{dx}\right)^2} \cdot \frac{\left(1+r\right)^3}{\left(1-r\right)^2}\left(\frac{1-r^2}{r^4} + \frac{1}{\left(1-r\right)^2}\right) \tag{39}$$

In the turbulent flow, the Nusselt number of the flowing geothermal fluid in the annular space of the coaxial pipes for heat transfer at the outer wall of annular duct was approximated as

$$Nu_a = 0.023 \operatorname{Re}_a^{0.8} \operatorname{Pr}^{0.4} \tag{40}$$

Substituting the equations (21) and (40) to (33), the following equation was obtained

$$\dot{S}'_{gen} = \frac{10.87\dot{m}C_p \mathrm{Re}_a^{0.2}\,\mathrm{Pr}^{0.6}\,D_o(1-r^2)}{T_m^2}\left(\frac{dT}{dx}\right)^2 + \frac{1.472\dot{m}^3\,\mathrm{Re}_a^{-0.2}}{\pi^2\rho^2 T_m D_o\left(1-r^2\right)^2}\cdot\zeta_{turb} \tag{41}$$

The following equation was obtained by expressing equation (41) in terms of the Reynolds number of the flow in the annular space and eliminating D_o

$$\dot{S}'_{gen} = \frac{13.84\dot{m}^2 C_p\,\mathrm{Pr}^{0.6}}{T_m^2\mu\,\mathrm{Re}_a^{0.8}}\left(1-r\right)\left(\frac{dT}{dx}\right)^2 + \frac{0.0446\,\mathrm{Re}_a^{4.8}\,\mu^5\zeta_{turb}}{T_m\rho^2\dot{m}^2}\left(1+r\right)^5 \tag{42}$$

Similarly, equation (42) can be minimized respect to the mass flow rate of geothermal fluid to obtain minimum entropy generation. The optimal mass flow rate of the geothermal fluid was determined under turbulent flow conditions as

$$m_{opt,turb} = 0.238\,\mathrm{Re}_a^{1.4}\,\chi_{turb}^{0.25} \tag{43}$$

where,

$$\chi_{turb} = \frac{\mu^6 T_m}{\rho^2 C_p\,\mathrm{Pr}^{0.6}\left(\frac{dT}{dx}\right)^2}\cdot\frac{\left(1+r\right)^5}{1-r}\left[\frac{(1+\mathrm{r})^{-0.2}\left(1-r^2\right)^2}{r^{4.8}} + \frac{1}{1-r}\right] \tag{44}$$

2.3 First- and second-law efficiencies analysis

The First- and Second-law efficiency are vital in designing, optimizing and modeling power plants. The First-law efficiency represents the efficiency of converting heat into work of the power plant. Whereas, the Second-law efficiency accounts for the system's inefficiency in terms of exergy destruction, the degradation of the system's ability to perform work with respect to its surroundings.

First- and Second- law efficiencies (or energy and exergy efficiencies) are generally defined as

$$\eta_I = \frac{\text{net work output}}{\text{total energy inputs}} \tag{45}$$

$$\eta_{II} = \frac{\text{net work output}}{\text{total exergy inputs}} \tag{46}$$

The mass, energy and exergy balances for any control volume at steady state with negligible kinetic and potential energy changes is given, respectively, as

$$\sum \dot{m}_{in} = \sum \dot{m}_{out} \tag{47}$$

$$\dot{Q} - \dot{W} = \sum \dot{m}_{out}h_{out} - \sum \dot{m}_{in}h_{in} \tag{48}$$

$$\dot{E}_{heat} - \dot{W} = \sum \dot{E}_{out} - \sum \dot{E}_{in} + \dot{E}_D \tag{49}$$

where $\dot{W}$ and $\dot{Q}$ are the rate of work transfer and rate of heat transfer, $\dot{E}_D$ is the rate of exergy destruction, and $\dot{E}_{heat}$ is the net exergy transfer by heat at temperature *T*, which is expressed as

$$\dot{E}_{heat} = \sum\left(1-\frac{T_o}{T}\right)\dot{Q} \tag{50}$$

The specific flow exergy and the rate of total exergy are determined by

$$e = h - h_0 - T_0(\mathrm{s}-\mathrm{s}_0) \tag{51}$$

$$\dot{E} = \dot{m}e \tag{52}$$

The subscript 0 is related to the restricted dead state and T_0 is the dead state temperature.

3. RESULTS AND DISCUSSION

3.1 Numerical results

The optimal mass flow rate of the geofluid was plotted against the flow regime in Fig. 2 with variation in gradient temperature (Fig. 2a) and geothermal heat source (Fig. 2b). Both two figures show an increase in optimal mass flow rate with the increase in Reynolds number. The Fig. 2(a) illustrates the higher underground gradient temperature the smaller optimum mass flow rate for a given inlet heat source and rejection temperature of 160ºC and 50ºC, respectively. It can be explained by increasing the underground gradient also getting the higher inlet source temperature. In the Fig. 2(b), the geothermal rejection temperature and the ground gradient temperature were fixed at 50°C and 3.6°C/100m, respectively. This figure illustrates the lower heat source inlet temperature the higher geofluid mass flow rate is required for given net power output.

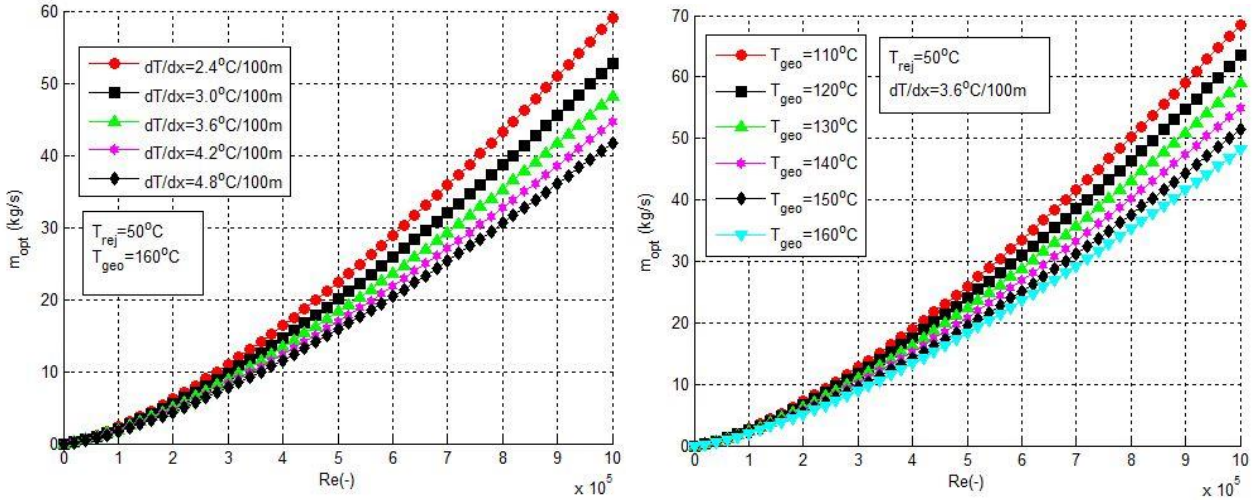

(a) (b)

Fig 2: Optimal mass flow rate of the geothermal fluid respect to flow regime and temperature gradient

The optimal outer pipe diameter respect to flow regime is shown in Fig. 3. The Fig. 3 (a) indicates that the higher underground gradient temperature the smaller size of the coaxial heat exchanger is required. Fig. 3 (b) illustrates an increase of coaxial heat exchanger diameter is result of increase in flow regime and decrease of geothermal inlet temperature. Hence, the size of pipes can be minimized as increase the geothermal inlet temperature or gradient temperature.

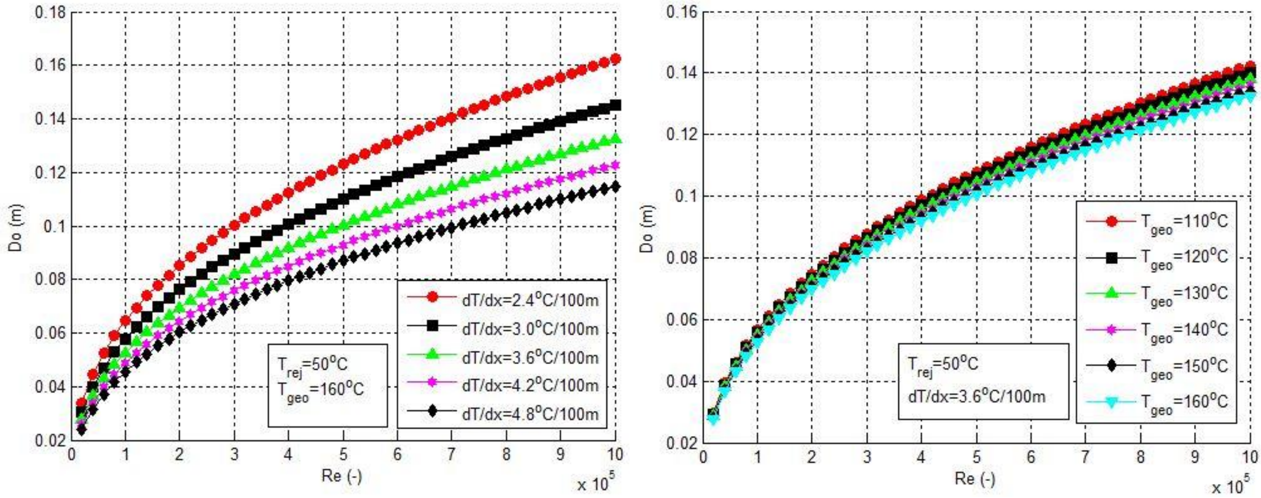

(a) (b)

Fig 3: Optimal coaxial heat exchanger outer diameter respect to flow regime and temperature gradient

Fig. 4a and Fig. 4b show the minimum entropy generation per unit length against the inlet flow regime with variation in ground gradient temperature and geothermal source inlet temperature. As shown in Fig. 4a, the energy destruction is not significantly different with various ground gradient temperature when the geofluid flows with small Reynolds number regimes. However, it is significantly deferent when the geofluid operating in large number of Reynolds number regimes. The entropy generation minimization can be decrease approximately 2 times if the ground gradient temperature increase from 2.4°C/100m to 4.8°C/100m. Similarly, the Fig. 4b illustrates that the entropy generation per unit length is decrease nearly two times by increasing the geofluid heat source from 110°C to 160°C.

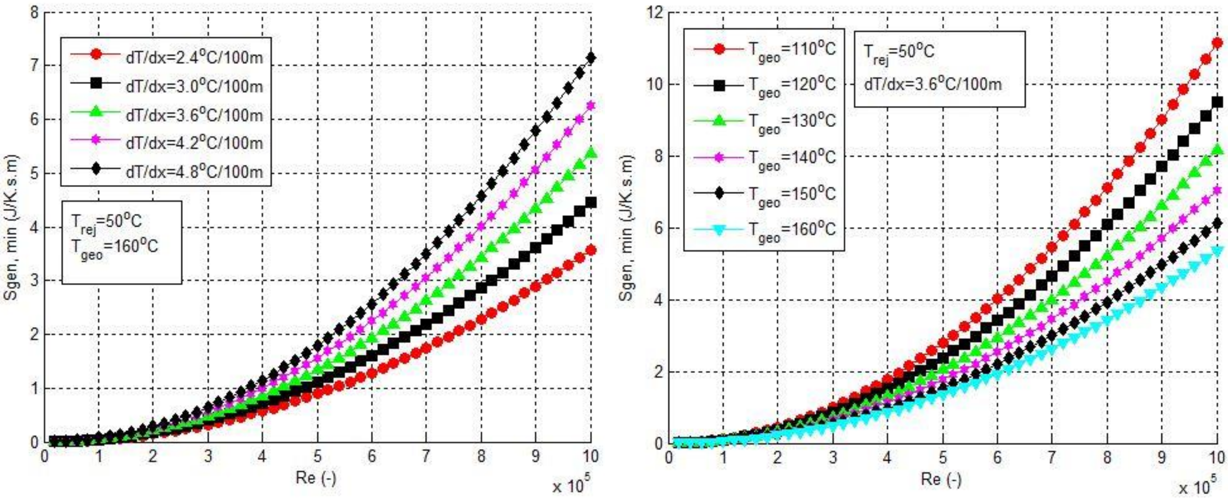

(a) (b)

Fig 4: Minimum entropy generation per unit length respect to flow regime and with variation in temperature gradient.

3.2 Case study

(a) Case study 1: Nigorikawa binary geothermal power plant

The Nigorikawa binary power plant was built by Japanese near Hakodate on Hokkaido. This plant was rated at 1000kW used a simple binary cycle with R114 was be chosen as working fluid (see Fig. 5). Table 1 gives the specifications of the plant [13].

Table 1: Operating data for Nigorikawa binary geothermal power plant [13]

Item	Fluid	Data
Turbine data	R114	
Rated capacity (kW)	R114	1000
Inlet pressure (MPa)	R114	1.343
Inlet temperature (K)	R114	98.5
Exhaust pressure (MPa)	R114	0.235
Exhaust temperature	R114	
Mass flow rate (kg/s)	R114	59.446
Brine inlet temperature (K)	Water	140
Brine outlet temperature (K)	Water	92
Mass flow rate (kg/s)	Water	49.996
Dead-stead temperature (K)		13

From these data given in table 1, it is easy to calculate the First Law efficiency of the power plant:

$$\eta_I = \frac{\dot{W}_{net}}{\dot{Q}_{in}} = \frac{\dot{W}_{net}}{\dot{m}_{geo}(\mathrm{h}_{in} - \mathrm{h}_{out})} = \frac{1000}{49.996 \times (589.13 - 385.33)} = 0.0981 \tag{53}$$

The exergetic efficiency of the plant

$$\eta_{II} = \frac{\dot{W}_{net}}{\dot{E}_{in}} = \frac{\dot{W}_{net}}{\dot{m}_{geo} e_{geo,in}} = \frac{1000}{49.996 \times 92.86} = 0.215 \tag{54}$$

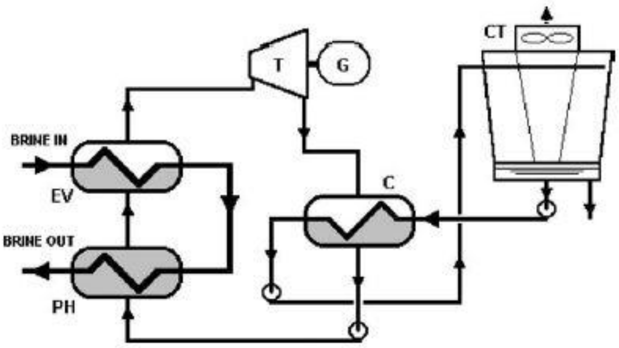

Fig. 5: Nigorikawa binary power plant [13]

The value of 9.81% and 21.6% of thermal efficiency and exergic efficiency, respectively, show that this power plant had efficiencies typical of binary plants.

(b) Case study 2: The Chingshui geothermal power plant [14]

The Chingshui, located in Yi-Lan County, northeastern of Taiwan (Republic of China), is one of the most promising geothermal resource in Taiwan. The schematic of the power plant is shown in Fig. 6 and the actual operating data from Chingshui plant is shown in Table 3 and Table 4.

Table 3: The operating data for Chingshui binary geothermal power plant [14]

Item	Fluid	Data
Working fluid inlet temperature (°C)	R134	128.8
Working fluid inlet pressure (MPa)	R134	4.413
Working fluid outlet temperature (°C)	R134	55.1
Working fluid outlet pressure (MPa)	R134	0.755
Working mass flow rate (kg/s)	R134	15.83
Water condenser outlet temperature (°C)	R134	33.
Brine inlet temperature (°C)	Water	155
Brine outlet temperature (°C)	Water	60.
Brine mass flow rate (kg/s)	Water	9.722
Brine heat source (kW)	Water	3642
Dead state temperature (°C)		13.

From these data, it is ease to determine the exergic efficient of the power plant:

$$\eta_{II} = \frac{\dot{W}_{net}}{\dot{E}_{in}} = \frac{\dot{W}_{net}}{\dot{m}_{geo} e_{geo,in}} = \frac{479}{9.722 \times 112.91} = 0.4364 \quad (55)$$

Table 4: Thermodynamics properties of working fluid in the Chingshui power plant

State No.	Fluid	Pressure (MPa)	Temperature (°C)	Mass flow rate (kg/s)	Enthalpy (kJ/kg)	Entropy (kJ/kg K)
1	R134	4.413	128.8	15.83	324.20	0.9793
2	R134	0.755	55.1	15.83	292.60	1.0030
3	R134	0.755	29.3	15.83	92.54	0.3445
4	R134	4.413	32.8	15.83	97.62	0.3511

The Second Law efficiency of 43.64% is very high exergy conversion efficiency of binary plant. It should be mentioned that the high geothermal inlet temperature and pressure giving a relatively high value for the incoming exergy.

However, the First Law efficiency of this power plant is not very impressive although of high exergic efficiency:

$$\eta_{I} = \frac{\dot{W}_{net}}{\dot{Q}_{in}} = \frac{\dot{W}_{net}}{\dot{m}_{geo}(\mathrm{h}_{in} - \mathrm{h}_{out})} = \frac{404.9}{3642} = 0.1112 \quad (56)$$

It should be emphasized that no preheater is be used in this power plant. The geothermal fluid outlet returns the underground in relatively high temperature.

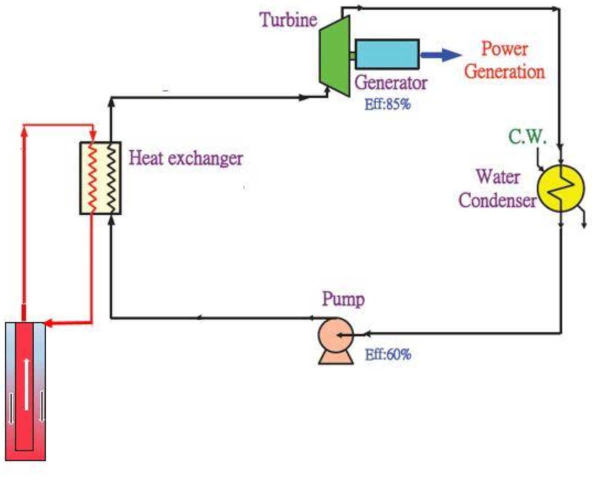

Fig 6: Chingshui binary geothermal power plant.

4. CONCLUSION

The thermal performance of a binary geothermal power plant was considered in this study. The entropy generation minimization analysis was conducted to observe the effects of heat transfer irreversibility and fluid friction irreversibility. The numerical results show that both the heat transfer irreversibility and fluid friction irreversibility result to the destruction of energy. The coaxial pipes diameters and the geofluid mass flow rate was optimized to obtain the minimum pumping power requirement and the energy destruction by the heat transfer and fluid friction irreversibilities. It was illustrated that the higher geothermal fluid temperature go to the evaporator minimize both the size of the downhole coaxial heat exchanger and the mass flow rate required to supply heat to the evaporator for the given net power. The first- and second-law efficiencies was analytically conducted to observe the thermal performance of the geothermal power plant. The two actual geothermal power plant given by the literature was considered in the case study to access the analysis. Both the analytical and actual models show that the first- and second-law efficiencies can be maximized by increasing the inlet geofluid resource temperature and decreasing the geothermal fluid rejection temperature.

5. ACKNOWLEDGEMENTS

The authors would like to acknowledge the Taiwan Ministry of Science and Technology for their supports to this study. This study is supported by the Taiwan National Science Council under grant MOST 103-3113-M-002-003.

Nomenclature		**Subscripts**	
C_p	Specific heat capacity, J/kgK	0	dead-state
D	Pipe diameter, m	a	annular space
e	Specific exergy, J/kg	D	Destruction
E	Exergy, W	gen	generation
f	Friction factor	geo	geothermal
h	Enthalpy, J/kg	i	inner
k	thermal conductivity, W/mK	I	first law
L	Length of the downhole pipes, m	II	second law
$\dot{m}$	Mass flow rate, kg/s	in	inlet
Nu	Nusselt number	lam	laminar flow
P	Pressure, Pa	m	mean
Pr	Prandtl number	min	minimum
Q	Heat, J	net	net
r	Diameter ratio	o	outer
Re	Reynolds number	opt	optimum
s	Specific entropy, J/kg.K	out	outlet
$\dot{S}$	Entropy generation rate, W/K	q	heat transfer
$\dot{S}'$	Entropy generation rate per unit length, W/m.K	rej	rejection
$\dot{S}'_{gen,\Delta T}$	Entropy generation rate related to heat transfer irreversibility, W/m.K	turb	turbulent flow
$\dot{S}'_{gen,\Delta P}$	Entropy generation rate related to fluid friction irreversibility, W/m.K	w	wall
t	time, s	W	work transfer
T	Temperature, oC		
V	Velocity, m/s		
W	Work		
x	axial distance along the pipe, m		
Greek symbols			
α	convection heat transfer coefficient, W/m2K		
ρ	density, kg/m3		
ζ	diameter ratio function		

Δ	difference
η	efficiency, %
μ	dynamic viscosity, Pa.s
χ	mass flow parameter

6. REFERENCES

[1] Barbier E (2002) Geothermal energy technology and current status an overview. *Renewable and Sustainable Energy Reviews*, vol. 6, pp. 3-65.

[2] Bertani R (2005) World geothermal power generation in the period 2001–2005. *Geothermics*, vol. 34, pp. 651–690.

[3] Chen F, Lu S M, Wang E, Tseng K T (2010) Renewable energy in Taiwan. Renewable and Sustainable Energy Reviews, vol. 14, pp. 2029–2038.

[4] Lee C S, P.T. Chang and J.B. Hsu (1981) A model approach for the geothermal fields in the slate terrain of Taiwan. In Geothermal Resources Council, TRANSACTIONS Vol. 5.

[5] DiPippo R, 2008. Geothermal Power Plants Principles, Applications Case Studies and Environmental Impact, 2nd edition. Butterworth-Heinemann, New York, NY, USA.

[6] Yari M (2010) Exergy analysis of various types of geothermal plants. *Renewable Energy,* vol. 35, pp. 112–121.

[7] Lim J S, Bejan A and Kim J H (1992) Thermodynamics of energy extraction from fractured hot dry rock. *Int. J. Heat and Fluid Flow,* Vol. 13, pp. 71-77.

[8] Franco A, Villani M (2009) Optimal design of binary cycle power plants for water-dominated, medium-temperature geothermal fields. *Geothermics,* vol. 38, pp. 379–391.

[9] Yekoladio P J, Bello-Ochende T and Meyer J P (2013) Design and optimization of downhole coaxial heat exchanger for an enhanced geothermal system (EGS). *Renewable Energy*, vol. 55, pp. 128-137.

[10] Bejan A, Tsatsaronis G, Moran M (1996) Thermal design and optimization. John Wiley & Sons, Canada.

[11] White F M (2003) Fluid mechanics, 5th edn. McGraw-Hill, New York.

[12] Incropera F P, De Witt D P (1990) Fundamentals of heat and mass transfer. John Wiley & Sons, Canada.

[13] Dipippo (2004) Second Law assessment of binary plants generating power from low-temperature geothermal fluids. *Geothermics,* vol. 33, pp. 565-586.

[14] Ko J W, Chen W R, Tsai M C, Hong C T, Chang J T, Shen J C, Chen D L, Hu S T (2012) The application of two-circulation generation technique on the geothermal generation. *Journal of Petroleum*, vol. 48, pp. 51-64. (in Chinese)